Engineering 3 (2017) 567–574

Contents lists available at ScienceDirect

Engineering

journal homepage: www.elsevier.com/locate/eng

Research
Green Chemical Engineering—Review

Insights into the Organotemplate-Free Synthesis of Zeolite Catalysts

Yeqing Wang, Qinming Wu, Xiangju Meng, Feng-Shou Xiao*

Key Lab of Applied Chemistry of Zhejiang Province, Department of Chemistry, Zhejiang University, Hangzhou 310007, China

ARTICLE INFO

Article history:
Received 24 October 2016
Revised 15 June 2017
Accepted 21 June 2017
Available online 18 July 2017

Keywords:
Zeolite seed-directed synthesis
Organotemplate-free synthesis
Zeolite seeds solution
Si/Al ratios
Zeolite micropore volume

ABSTRACT

As the most important nanoporous material, zeolites, which have intricate micropores, are essential heterogeneous catalysts in industrial processes. Zeolites are generally synthesized with organic templates under hydrothermal conditions; however, this method is environmentally unfriendly and costly due to the formation of harmful gases and polluted water. This article briefly summarizes the role of organic templates and describes designed routes for the organotemplate-free synthesis of zeolites, aided by zeolite seeds and zeolite seeds solution. Furthermore, this review explicates that the micropore volume decreases with an increase of the Si/Al ratios in the organotemplate-free synthesis of zeolite products, where Na^+ exists as an alkali cation. This feature is very important in directing the synthesis of zeolite catalysts with controllable Si/Al ratios under organotemplate-free conditions, and is thus important for the efficient design of zeolites.

1. Introduction

Zeolites with crystalline micropores (0.3–1.5 nm) are the most important nanoporous materials, and have been widely used as ion-exchangers, sorbents, and catalysts [1–11]. At present, zeolites are extensively and widely used due to the suitable sizes of their channels and cavities [12]. For example, zeolites have been successfully used in drug delivery systems [13–15]. The synthesis of zeolites is usually carried out hydrothermally, starting from silicate or aluminosilicate gels in alkaline media and with temperatures ranging from 60 °C to 200 °C [16–21]. In the early stages, the synthesis of zeolites with faujasite (FAU), Linde-type L, and mordenite structures was performed in aluminosilicate gels containing inorganic cations, such as sodium (Na^+) and potassium (K^+) cations, as structure-directing agents (SDAs) [21–27]. Later, organic cations such as quaternary ammonium were introduced into the synthetic systems as organic structure-directing agents (OSDAs), leading to the formation of a series of novel zeolite structures. ZSM-5 and beta zeolites are typically and successfully synthesized with the use of tetrapropylammonium and tetraethylammonium (TEA), respectively [28–33]. Compared with inorganic cations, the use of OSDAs has obvious disadvantages: ① OSDAs are expensive, so the resulting zeolite products are always costly; ② high-temperature combustion is required to remove organic templates by destroying these organic components, and produces harmful gases such as nitrogen oxides (NO_x) and carbon dioxide (CO_2); ③ the use of OSDAs produces a large amount of polluted water, and is thus environmentally unfriendly; and ④ the associated energy released by burning OSDAs, in combination with the formed water, can be extremely detrimental to the inorganic structure of the zeolites [34,35]. These shortcomings undoubtedly hinder the practical application of OSDAs. The best solution to these issues is to realize the organotemplate-free synthesis of zeolites, in order to completely avoid the combustion of costly OSDAs. Fortunately, this concept was shown to be very successful in the synthesis of aluminum (Al)-rich ZSM-5 zeolite, in which Na^+ can serve as the SDA [36–40]. Since this milestone was achieved, the industrial applications of the ZSM-5 zeolites have been significantly enhanced. However, the organotemplate-free synthesis of other zeolites, which normally requires the assistance of OSDAs, remains a challenge. For example, although beta zeolite exhibits excellent catalytic properties, its organotemplate-free synthesis was unsuccessful until 2008 [41]. In this review, we briefly summarize the general strategies to

* Corresponding author.
E-mail address: fsxiao@zju.edu.cn

http://dx.doi.org/10.1016/J.ENG.2017.03.029

synthesize zeolite catalysts, and provide insights into hydrothermal crystallizations under organotemplate-free conditions.

2. Understanding the major role of organic templates and designing organotemplate-free strategies for the synthesis of zeolite catalysts

As a typical example, Fig. 1(a) [42] shows the crystallization curves of pure silica MFI zeolite synthesized with and without tetrapropylammonium cations (TPA^+). If there is no TPA^+ in the starting aluminosilicate gel, the zeolite cannot be obtained. However, if the starting aluminosilicate gel contains TPA^+, perfect MFI crystals are prepared. These results suggest that TPA^+ is an excellent OSDA for the formation of MFI crystals. This crystallization curve mainly includes the two steps of ① induction and ② crystal growth. The turning point between induction and crystal growth corresponds with the formation of zeolite nuclei (i.e., nucleation). It is notable that the induction step takes a much longer time than the crystal growth step, which indicates that once the nuclei are formed, the zeolite products crystallize quickly. These results indicate that nucleation plays a critical role in the crystallization of zeolites in the presence of TPA^+.

Davis et al. [43,44] systemically investigated the crystallization of zeolites in the presence of organic templates, and proposed that the crystallization involves two main activation energies: ① the formation of zeolite nuclei from the assembly of inorganic aluminosilicate species and OSDA cations, and ② the crystal growth from the zeolite nuclei (Fig. 1(b)). Interestingly, they suggested that the OSDAs could be encapsulated by inorganic silicate/aluminosilicate species, and that the activation energy of the formation of zeolite nuclei was larger than that of the crystal growth.

Based on this knowledge and understanding, it is suggested that the major role of the OSDAs in zeolite synthesis is to form the zeolite nuclei. It is possible that the OSDAs are already encapsulated with silicate/aluminosilicate species once the zeolite nuclei have formed. Therefore, it is difficult for the OSDAs to influence crystal growth. If this is so, then OSDAs are not necessary for the growth of zeolite crystals, and the organotemplate-free synthesis of zeolites could be implemented by the introduction of zeolite nuclei into the starting aluminosilicate gels.

Two strategies to introduce zeolite nuclei into the starting aluminosilicate gels for the synthesis of zeolite catalysts were recently designed, involving the employment of zeolite crystals as seeds (i.e., zeolite seeds) and zeolite seeds solution. Although zeolite seeds solution generally has no X-ray diffraction (XRD) peaks that are associated with zeolite structures, it has obvious infrared radiation (IR) and Raman bands that are associated with zeolite building units [45–47].

3. Organotemplate-free synthesis in the presence of zeolite seeds

As the first example of the organotemplate-free synthesis of zeolites, Xie et al. [41] reported that beta zeolite could be successfully crystallized from aluminosilicate gels with the assistance of zeolite seeds, and without the addition of an organic template (Fig. 2). The XRD pattern of the product indicated the successful synthesis of beta zeolite, as it contained characteristic peaks associated with the BEA zeolite structure. The scanning electron microscopy (SEM) image of the BEA zeolite showed almost uniform morphology of the crystals, with a crystal size of 100–160 nm. In addition, the nitrogen isotherms of the BEA zeolite product demonstrated that the beta zeolite already had opened micropores, leading to a thorough avoidance of the combustion of the BEA zeolite. In particular, the results showed a good relationship between the sample crystallinity and the crystallization time, which ranged from 2 h to 20 h, indicating that the induction step in the organotemplate-free synthesis was significantly reduced compared with that in the conventional synthesis of beta zeolite using organic templates.

The crystallization of beta zeolite under organotemplate-free conditions was investigated by high-resolution transmission electron microscope (HRTEM). It was found that zeolite seeds, which act as the "core," gradually grow until there is full consumption of the amorphous aluminosilicate gel. Finally, a core-shell structure of beta zeolite is formed [41,48]. Because the zeolite seeds direct the crystallization of the beta zeolite without the addition of an organic template, this route is referred to as seed-directed synthesis (SDS) by the authors.

The important factors in the organotemplate-free and SDS of beta zeolite (beta-SDS) were systemically investigated, and it was shown that the amount and type of beta zeolite seeds are critical for the crystallization of the beta-SDS sample. Through optimization, a beta-SDS sample was obtained with high crystallinity and large surface area (BET specific surface area 655 $m^2 \cdot g^{-1}$), by the addition of a small amount of beta zeolite seeds (as low as 1.4 wt%) at 120 °C [49]. In addition, it is notable that although beta-SDS initially has a relatively low yield, its yield is remarkably enhanced by the use of a precursor suspension with a high Al content, as recently reported by Otomo and Yokoi [50]. In 2009, Majano et al. [51] presented the synthesis of Al-rich beta zeolite in the presence of beta zeolite seeds without calcination. These researchers emphasized that the Si/Al ratio in the Al-rich beta zeolite was similar to that in the natural counterpart of beta zeolite, the mineral tschernichite, which has a Si/Al ratio as low as 3.9 [52–54]. In contrast, the Si/Al ratios in the beta zeolites that were templated using OSDAs range from about 12

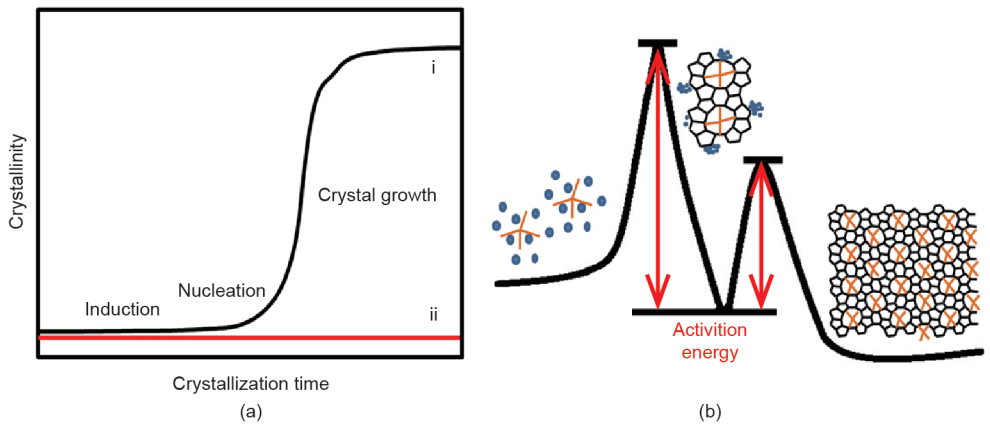

Fig. 1. (a) X-ray crystallization curve of pure silica MFI zeolite synthesized (i) with and (ii) without TPA^+ (reprinted with permission from Ref. [42], © 2016 Wiley); (b) scheme for the crystallization of zeolites synthesized with organic templates.

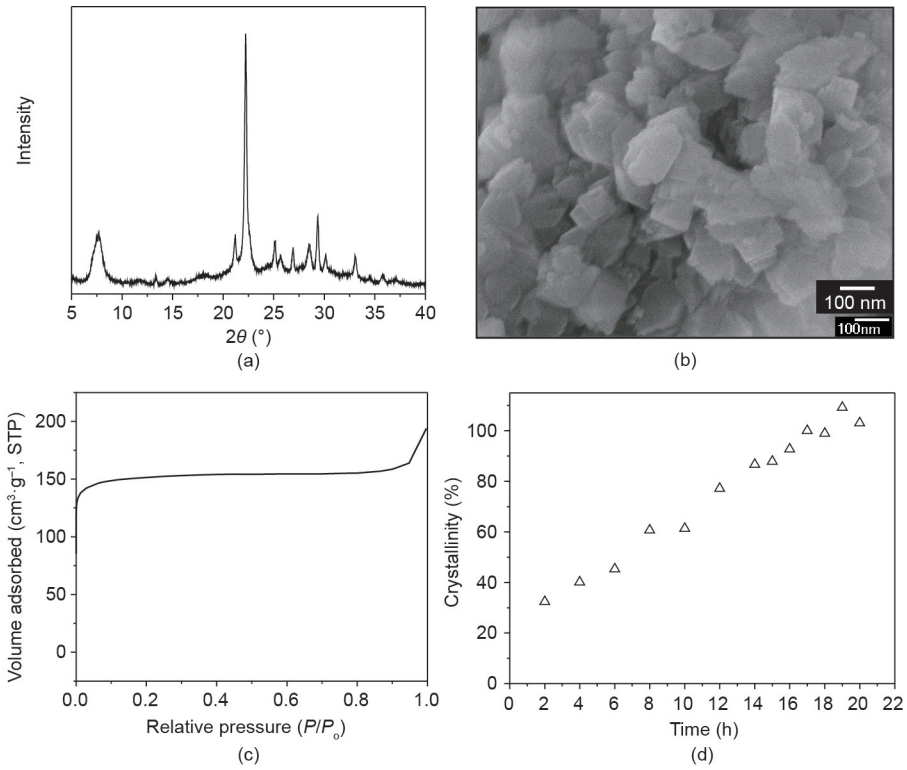

Fig. 2. (a) The XRD pattern, (b) SEM image, and (c) nitrogen isotherms of the as-synthesized beta-SDS sample; (d) the dependence of sample crystallinity on crystallization time for the beta-SDS sample. The sample of as-synthesized beta-SDS that crystallized at 17 h was denoted as 100% crystallinity. Beta-SDS: seed-directed synthesis of beta zeolite. (Reprinted with permission from Ref. [41], © 2008 American Chemical Society)

to ∝ [55–61]. It is very interesting to note that the Al-rich beta-SDS sample has excellent thermal and hydrothermal stabilities. For example, the crystallinity of the beta-SDS sample was essentially constant after 100% steaming treatment at 750 °C for 8 h, while it markedly decreased if the beta zeolite was synthesized with TEA (beta-TEA). These results may indicate that the beta-SDS sample had much less defects than the conventional beta-TEA sample [48]. Because it results in rich Al species and excellent stabilities, the beta-SDS offers a new platform for the future development of efficient zeolite catalysts that require a high acidic density.

In 2010, Kamimura et al. [62] reported the OSDA-free synthesis of beta zeolite, which was performed by using a small amount of beta zeolite seeds and carefully adjusting the synthetic parameters. The Si/Al ratios of the product were 5.2–6.8. In addition, further crystallization of beta zeolite was successfully achieved in the presence of the OSDA-free beta crystals, which acted as renewable seeds, resulting in a completely OSDA-free process for the synthesis of beta zeolite; this process was named "green beta," as shown in Fig. 3.

In 2009, Yokoi et al. [63] reported the successful organotemplate-free synthesis of RTH-type zeolite by the addition of zeolite seeds; this product was designated as TTZ-1 zeolite. RTH-type zeolite is normally templated from 1,2,2,6,6-pentamethylpiperidine cations and *N*-ethyl-*N*-methyl-5,7,7-trimethylazoniumbicyclo[4.1.1]octane. [Al, B]-TTZ-1 and [Ga, B]-TTZ-1, as RTH-type zeolites, can also be obtained using the organotemplate-free route. More importantly, these TTZ-1 zeolites showed excellent catalytic properties in methanol-to-olefins (MTO) reactions, and are thus potentially important for the development of highly efficient MTO catalysts [64,65].

It is noteworthy that the Si/Al ratios of the TTZ-1 zeolite can be adjusted from 79 to 200, although it is difficult to realize the organotemplate-free synthesis of high-silica zeolites. However, this was successfully performed with the addition of boron (B) species in the starting aluminosilicate gels, such that both Al^{3+} and B^{3+} species could be incorporated into the zeolite framework. After deboronation, a TTZ-1 zeolite with a high Si/Al ratio was obtained; this process thus offers a novel route for the synthesis of high-silica RTH-type zeolite.

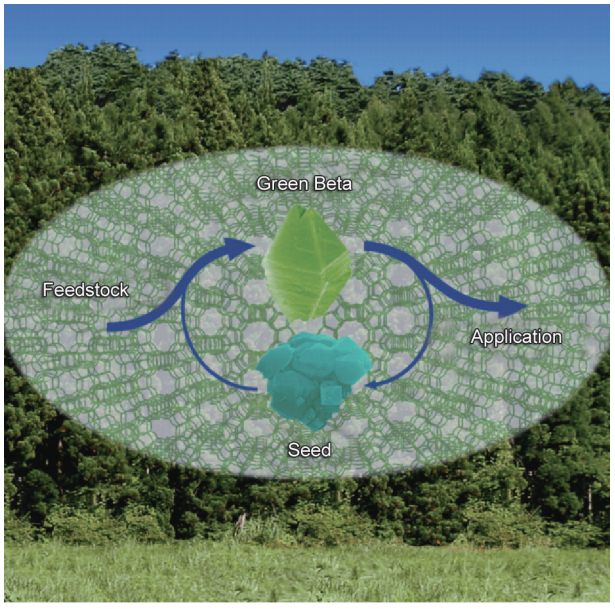

Fig. 3. The scheme for "green beta." (Reprinted with permission from Ref. [62], © 2010 Wiley)

In 2012, Okubo and coworkers extended this OSDA-free route to synthesize ZSM-5 and ZSM-11 zeolites with three-dimensional 10-membered ring (MR) openings, MTW zeolite with one-dimensional 12MR openings [66,67], and ferrierite zeolites with two-dimensional 10MR and 8MR openings [68]. All of these zeolites were relatively rich in Al species in the zeolite framework, compared with

the corresponding zeolites synthesized using organic templates. For example, the SDS of ZSM-11 zeolite resulted in a Si/Al ratio of just 8.3, while the typical Si/Al ratio of the product of the ZSM-11 zeolite synthesis using organic templates was as high as 33. More Al species in the zeolite frameworks will be efficient for catalytic conversions over the zeolite catalysts, which require a high acidic density (e.g., cracking catalysts).

In 2012, Zhang et al. [69] and Yang et al. [70] showed the organotemplate-free and SDS of levyne zeolite with 8MR openings (LEV-SDS) and ZSM-34 zeolite (ZSM-34-SDS) with an intergrowth of erionite and offretite structures, respectively. The Si/Al ratios in the LEV-SDS and ZSM-34-SDS zeolite were about 3.8–4.1, which are much lower than those of the corresponding zeolites synthesized with organic templates. The H-form of ZSM-34-SDS zeolite had an excellent selectivity to propylene (55.2%), which was even better than that of the industrial SAPO-34 catalyst (47.0%) [70].

In 2014, MTT and TON zeolites with one-dimensional 10MR openings were successfully achieved under organotemplate-free and seed-directed conditions [71,72]. These two zeolites exhibited excellent performance for the isomerization of *m*-xylene to *p*-xylene and for the dewaxing of diesel; until this point, organic templates had been necessary in their synthesis [73,74]. By employing a seed-directed route, high-silica MTT and TON zeolites were successfully prepared, and designated as ZJM-6 and ZJM-4 zeolites, respectively. The H-form of ZJM-6 zeolite exhibits a higher activity in *m*-xylene isomerization, compared with the conventional ZSM-23 zeolite synthesized with an organic template.

To illustrate the role of zeolite seeds, Fig. 4 [71] compares the crystallization curves for ZJM-6 zeolite, ZSM-23 zeilite templated from *N*,*N*-dimethylformamide (DMF) (ZSM-23-D), and ZSM-23 zeolite synthesized with both DMF and ZSM-23 seeds (ZSM-23-S) at crystallization temperatures of 150–170 °C. In general, there are two steps in the hydrothermal synthesis of zeolites: induction and crystallization. However, there was almost no induction period in the synthesis of ZJM-6 zeolite (curves i in Fig. 4). In contrast, the induction period is as long as 12–34 h when the organic template is present for the synthesis of ZSM-23-D (curves iii in Fig. 4). The induction period is obviously shortened if the synthesis of ZSM-23-S occurs in the presence of DMF and ZSM-23 seeds, but it still takes 6–15 h (curves ii in Fig. 4). Clearly, various samples (i.e., ZJM-6, ZSM-23-D, ZSM-23-S) had quite different induction periods under the same temperature. These results indicated that the role of zeolite seeds in the crystallization of ZJM-6 zeolite was to reduce the induction time, which is considered to be the rate-determining step in the organotemplate-free crystallization of zeolites [71].

Furthermore, samples with a series of heteroatoms in the zeolite framework were produced through the organotemplate-free syntheses of zeolites. Yokoi et al. [63,75] reported the introduction of heteroatoms such as B^{3+}, Ga^{3+}, and Fe^{3+} in the zeolite framework of RTH-type zeolite, and Xiao et al. [76,77] showed the incorporation of these heteroatoms into the zeolite framework of ZSM-34 and beta zeolites, respectively. Of these, the Fe-beta-SDS zeolite demonstrated superior catalytic properties in the direct decomposition of N_2O into nitrogen and oxygen, with the iron species serving as the active sites.

In 2011 and 2014, Sano and coworkers [78–81] demonstrated seeded interzeolite conversions from high-silica FAU into BEA, LEV, and MAZ-type zeolites in the absence of OSDAs. This process was an extension of the organotemplate-free and seed-directed route, in which the starting aluminosilicate gels were replaced by high-silica FAU zeolite. For example, FAU zeolite can successfully convert into LEV zeolite without the addition of an organic template in the presence of zeolite seeds under hydrothermal synthesis conditions, resulting in a unique core/shell structure of the LEV zeolite product [79].

In 2015, Goel et al. [82] reported synthetic protocols and guiding principles for the synthesis of zeolite crystals by means of interzeolite transformations with zeolite seeds, in the absence of OSDAs. High-silica daughter zeolites, such as MFI (ZSM-5), CHA (chabazite), STF (SSZ-35), and MTW (ZSM-12) zeolites, have been successfully obtained via interzeolite transformations from FAU or BEA parent zeolites; this process is based on the fact that the daughter materials have higher framework densities than the parent zeolite. In addition, nucleation and growth become possible in the presence of seeds or structural building units that are common to the parent and target structures under appropriate synthesis conditions (Fig. 5) [82].

As observed in the above examples, it is evident that the zeolite seeds in the starting aluminosilicate gels induce the crystallization of target zeolites under suitable hydrothermal conditions; the zeolite seeds are still detectable in the XRD patterns in the starting mixtures, even if the synthetic systems are strongly basic.

4. Organotemplate-free synthesis in the presence of zeolite seeds solution

In 1999 and 2000, Zhou et al. [45,46] reported the synthesis of beta zeolite with a relatively low Si/Al ratio (4–8) using zeolite seeds solution (2 wt%–8 wt% in total silica) without additional OSDAs. The zeolite seeds solution was prepared by heating aluminosilicate gels with a molar ratio of Al_2O_3/80SiO_2/2.5TEA^+/750H_2O at 140 °C for 4 h. Because it is difficult to characterize the structure of the zeolite seeds solution as a liquid, the zeolite seeds solution was assembled with surfactants to form a solid mesoporous material, which was relatively easy to characterize. It is interesting to note that the IR spectrum of this sample exhibits obvious bands at 520–600 cm^{-1}, which are associated with the zeolite building units [83]. In addition, the HRTEM image of the MAS-7 sample shows small ordered domains, which are associated with the existence of zeolite building

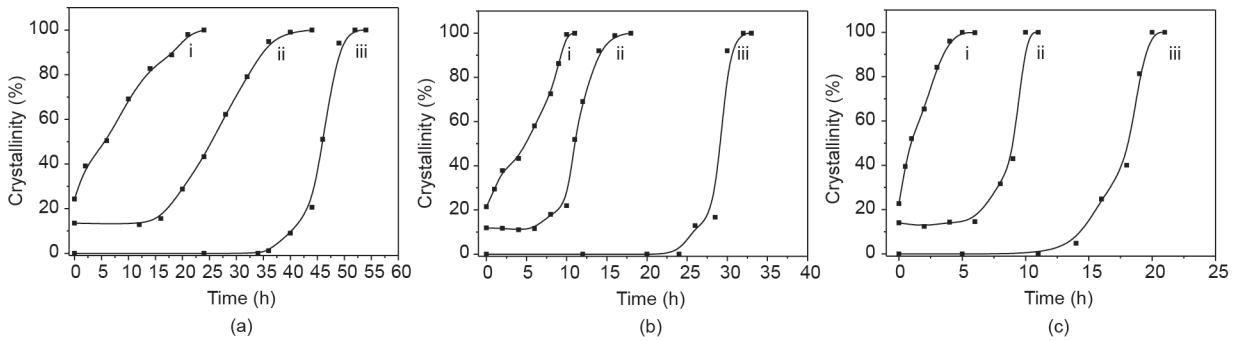

Fig. 4. The dependences of crystallinity on the crystallization time of (i) ZJM-6 zeolite, (ii) ZSM-23 zeolite synthesized in the presence of both DMF template and ZSM-23 seeds (ZSM-23-S), and (iii) ZSM-23 zeolite synthesized in the presence of DMF template (ZSM-23-D) at (a) 150 °C, (b) 160 °C, and (c) 170 °C, respectively. (Reprinted with permission from Ref. [71], © 2014 Elsevier)

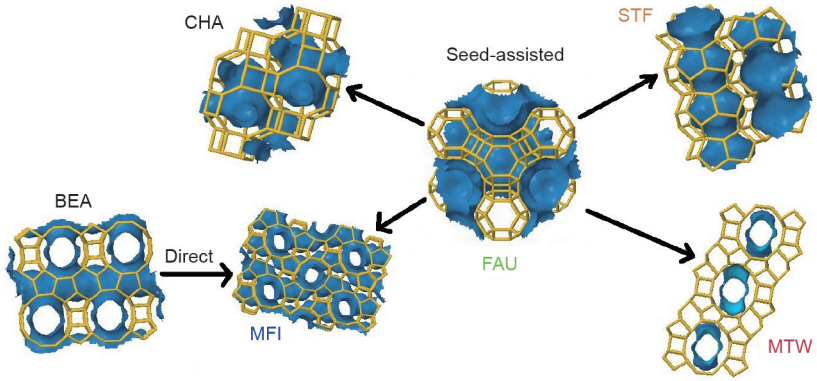

Fig. 5. Scheme for OSDA-free interzeolite transformations. (Reprinted with permission from Ref. [82], © 2015 American Chemical Society)

units (Fig. 6) [84]. These results indicate that the zeolite seeds solution contains zeolite building units.

In 2008, Wu et al. [85] demonstrated the organotemplate-free synthesis of ZSM-34 zeolite with high crystallinity in the presence of zeolite L seeds solution. ZSM-34 zeolite, which contains cancrinite (CAN) cages, enables excellent conversion of methanol to C_2–C_5 olefins, a process that is normally templated by choline and diamines [86–88]. The zeolite L seeds solution contained abundant zeolite building units of CAN cages, leading to the induction of ZSM-34 zeolite under organotemplate-free conditions [85].

In 2011, Zhang et al. [89] reported the organotemplate-free synthesis of high-silica ferrierite zeolite (FER structure) in the presence of RUB-37 zeolite seeds (CDO structure). There was a discrepancy between the structure of the target product and that of the zeolite seeds. High-silica ferrierite zeolite with 10MR and 8MR openings is normally achieved with the assistance of organic templates. The layered structures of CDO and FER zeolite are quite similar, and a shift of the layers in the horizontal direction was expected and observed, indicating that the zeolite building units of ferrierite zeolite and of RUB-37 zeolite were almost the same. It is worth noting that the XRD peaks related to the RUB-37 zeolite were undetectable after the RUB-37 zeolite seeds existed in the starting aluminosilicate gels for 12 h. However, after heating this synthetic system at 150 °C for 72–168 h, perfect high-silica ferrierite zeolite crystals were obtained. Zhang et al. [89] proposed and then demonstrated that the zeolite building units of the RUB-37 zeolite (CDO structure) could be implemented to induce the crystallization of the ferrierite zeolite (FER structure) without the addition of any organic template.

In order to acknowledge the role of RUB-37 zeolite seeds in the crystallization process, UV-Raman spectra of the amorphous starting aluminosilicate gels were performed in the presence and absence of the RUB-37 zeolite seeds (Fig. 7) [89]. There was an obvious peak at 430 cm^{-1} that was associated with the contribution of 5MRs from the CDO zeolite building units, which should result from the dissolution of RUB-37 zeolite seeds crystals [90]. This result was consistent with the suggestion that the FER zeolite nuclei are induced by the CDO zeolite building units.

In 2012, Kamimura et al. [67] introduced an organotemplate-free synthesis of MTW zeolite by the addition of beta zeolite seeds into the starting sodium aluminosilicate gels; in this case, the structures of the zeolite seeds and the zeolite product were obviously different. After a series of comprehensive investigations with various characterization techniques, it was suggested that the starting sodium aluminosilicate gels in the presence of the zeolite seeds provided specific aluminosilicate precursors with target zeolite building units to induce the nucleation of MTW zeolite prior to the spontaneous induction of other zeolites.

More recently, Iyoki et al. [91] presented the successful synthesis

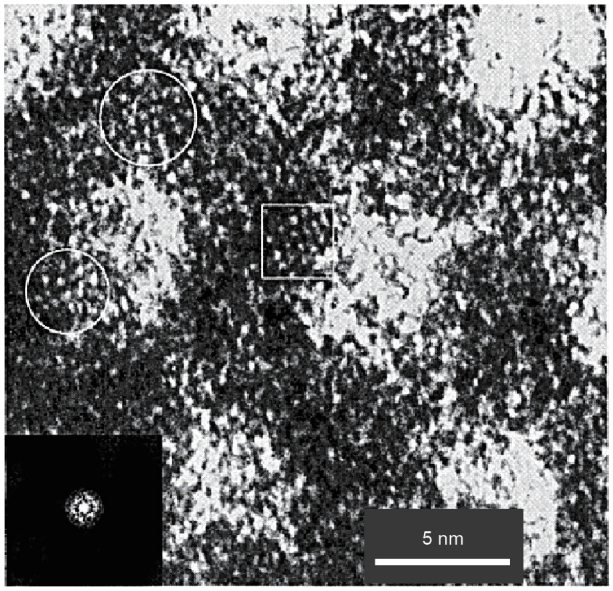

Fig. 6. HRTEM image of MAS-7 sample. Inset is the Fourier diffractogram of the square area. Other areas marked with circles present fairly ordered micropore arrays. (Reprinted with permission from Ref. [84], © 2002 American Chemical Society)

of NES-type zeolites from an organotemplate-free and SDS route in the presence of EUO-type crystals as zeolite seeds for the first time. They suggested that the less dense NES-type zeolite was kinetically favorable over the denser EUO-type zeolite under the same synthesis conditions. Therefore, the NES-type zeolite product was prepared rather than the EUO-type zeolite, even though the starting aluminosilicate gels contained EUO-type zeolite seeds. The NES- and EUO-type structures contained similar zeolite building units (Fig. 8) [91]; this was the critical factor for the induction of NES-type zeolite by the addition of EUO-type zeolite seeds. This economical and environmentally friendly synthesis approach for NES-type zeolite is expected to open up a new way to prepare green zeolite catalysts.

As discussed in the results above, it is clear that the zeolite building units are important for the induction of zeolite growth. Although zeolite building units are undetectable by XRD patterns, characteristic signals can be observed when using spectroscopic techniques such as IR and UV-Raman spectroscopy.

5. Dependences of Si/Al ratios and micropore volume in the organotemplate-free synthesis of zeolite catalysts

Fig. 9 provides a brief summary of the dependences of Si/Al

ratios and micropore volume in the organotemplate-free synthesis of zeolite catalysts using Na^+ as an alkali cation [62,66–68,71,89,92–94]. It is interesting to note that the zeolites with larger micropore volumes always have lower Si/Al ratios. In contrast, the zeolites with smaller micropore volumes always have higher Si/Al ratios. It is clear that the Si/Al ratios in the organotemplate-free synthesis of zeolites strongly rely on the micropore volume of the zeolite structures. It is reasonable to suppose that this kind of phenomena is related to the Coulomb force between the inorganic cations and the negative charges in the zeolite framework [95–97]. Zeolites with larger micropore volumes may contain more Na^+, which requires the presence of more negative charges in the zeolite framework to balance them. Considering that the incorporation of tetrahedral Al species in the zeolite framework is the only way to form a negative charge, it is reasonable for the zeolites with larger micropore volumes to be more Al rich, and for those with smaller micropore volumes to be less Al rich. For example, beta-SDS samples with micropore volumes of 0.2–0.22 $cm^3 \cdot g^{-1}$ have Si/Al ratios that range from 4 to 6.8 [62], while the ZSM-23 zeolite with a micropore volume of 0.046 $cm^3 \cdot g^{-1}$ has Si/Al ratios of 20–25 [71]. Thus, the Si/Al ratios in the zeolite products may be predictable from the micropore volume of the target structures.

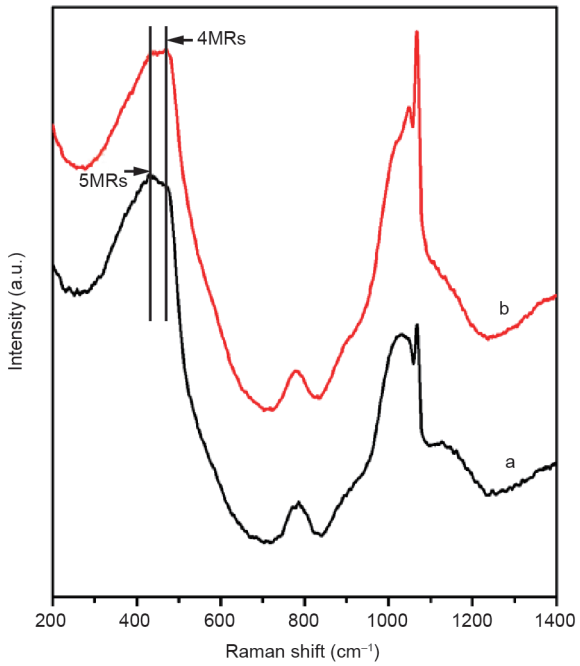

Fig. 7. UV-Raman spectra of the amorphous product at 12 h in the (a) absence and (b) presence of RUB-37 zeolite seeds. (Reprinted with permission from Ref. [89], © 2011 Royal Society of Chemistry)

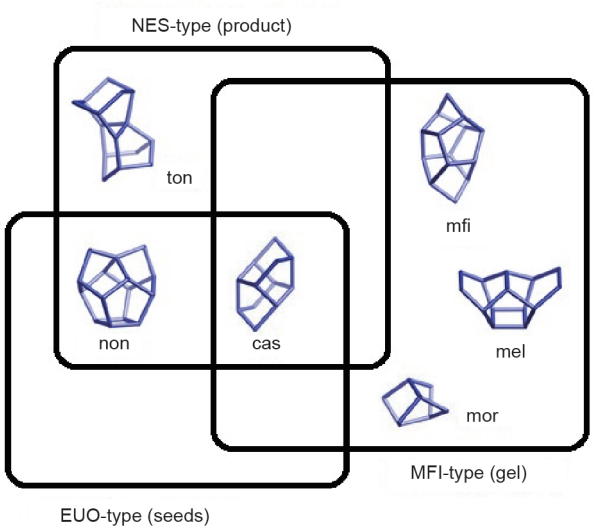

Fig. 8. Correlation of the composite building units in NES-, EUO-, and MFI-type zeolites. (Reprinted with permission from Ref. [91], © 2015 Elsevier)

Based on the dependences of the Si/Al ratios and micropore volume in the organotemplate-free synthesis of zeolite catalysts, it is suggested that larger sizes of inorganic cations occupy larger micropore volumes; this would significantly reduce the number of inorganic cations in the zeolite micropores, causing the zeolite product to have higher Si/Al ratios. At present, high-silica Cu-SSZ-13 with a CHA zeolite structure is an industrial catalyst for the selective catalytic reduction of NO_x with ammonia (NH_3); the high-silica SSZ-13 zeolite is generally synthesized with the addition of OSDAs [98–101]. To reduce the zeolite cost, the organotemplate-free and SDS of CHA zeolite has been performed; however, its Si/Al ratios are less than 4 [102], which is low for industrial applications. To increase the Si/Al ratios in the CHA zeolite product, Ren et al. [103] employed much larger inorganic cations (a Cu^{2+}-amine complex) to fill up the zeolite cages of the CHA zeolite structure. As expected, high-silica CHA zeolite with a Si/Al ratio higher than 5 was obtained using larger Cu^{2+}-amine cations; this product was designated as ZJM-1 zeolite (Cu-ZJM-1). Because the Cu^{2+}-amine cations contain copper species, Cu^{2+} ion exchange is not necessary to introduce copper species to the ZJM-1 zeolite. Cu-ZJM-1 exhibits excellent catalytic performance in the selective catalytic reduction of NO_x with NH_3 (Fig. 10) [103].

6. Conclusions and perspectives

This review emphasizes the role of zeolite nuclei in directing crystal growth and the cation filling of zeolite micropore volume under organotemplate-free conditions. The zeolite nuclei that are added in the starting aluminosilicate gels in the organotemplate-free route mainly come from zeolite crystals as seeds and from zeolite seeds solutions as zeolite building units. Under suitable conditions, if zeolite nuclei exist in the starting aluminosilicate gels and if the zeolite micropore volume can be sufficiently filled, the organotemplate-free synthesis of zeolite catalysts should be successful. This strategy completely avoids the combustion of costly OSDAs and the production of harmful gases and liquid wastes, so it is environmentally friendly and energy saving.

It is important to combine the organotemplate-free route with other sustainable approaches for the synthesis of zeolite catalysts.

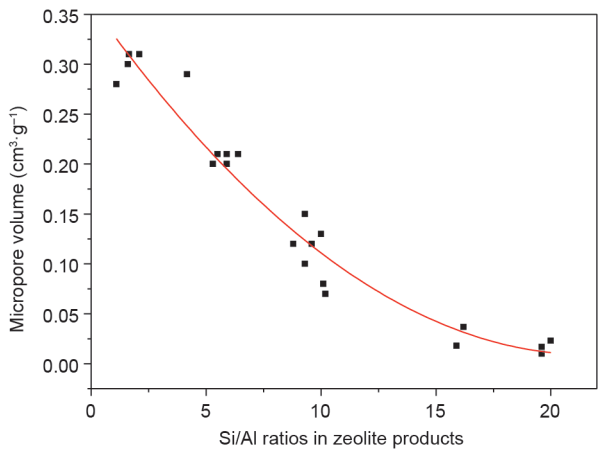

Fig. 9. A brief summary of the dependences of Si/Al ratios and micropore volume in the organotemplate-free synthesis of zeolite catalysts.

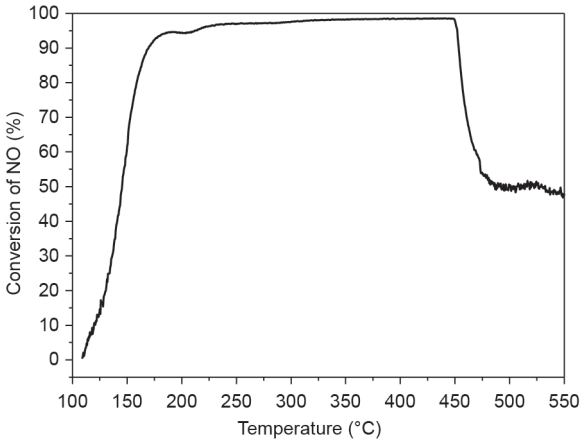

Fig. 10. Nitric oxide (NO) conversion profile for Cu-ZJM-1 at various temperatures. (Reprinted with permission from Ref. [103], © 2011 Royal Society of Chemistry)

For example, Wu et al. [104] demonstrated the sustainable synthesis of ZSM-5 and beta zeolite without the addition of organic templates or solvent. In that case, a large amount of polluted wastes was effectively avoided and the zeolite product yields were significantly improved. Chen et al. [105] reported the fast synthesis of zeolite A nanocrystals with no organic compounds under microwave radiation, and showed that the microwave radiation significantly improved the efficiency of the zeolite synthesis.

More recently, the organotemplate-free route has been extended to synthesize aluminophosphate-based molecular sieves. For example, Yu et al. [106–108] presented a facile organotemplate-free synthesis of JU93, JU102, and JU103 in an alkali system under hydrothermal conditions. It is reasonable to assume that more examples of the organotemplate-free synthesis of aluminophosphate-based molecular sieves will be realized in the future.

The sustainable nature of the organotemplate-free route is important for the industrial production of zeolite catalysts in the future. As a typical example, the German chemical company BASF SE has successfully commercialized the organotemplate-free synthesis of beta-SDS zeolite.

Acknowledgements

This work was supported by the National Natural Science Foundation of China (21273197 and 21333009).

Compliance with ethics guidelines

Yeqing Wang, Qinming Wu, Xiangju Meng, and Feng-Shou Xiao declare that they have no conflict of interest or financial conflicts to disclose.

References

[1] Iwamoto M, Yahiro H, Tanda K, Mizuno N, Mine Y, Kagawa S. Removal of nitrogen monoxide through a novel catalytic process. 1. Decomposition on excessively copper-ion-exchanged ZSM-5 zeolites. J Phys Chem 1991;95(9):3727–30.
[2] Corma A. Inorganic solid acids and their use in acid-catalyzed hydrocarbon reactions. Chem Rev 1995;95(3):559–614.
[3] Shelef M. Selective catalytic reduction of NO_x with N-free reductants. Chem Rev 1995;95(1):209–25.
[4] Pârvulescu VI, Grange P, Delmon B. Catalytic removal of NO. Catal Today 1998;46(4):233–316.
[5] Corma A, Forness V, Pergher SB, Maesen TLM, Buglass JG. Delaminated zeolite precursors as selective acidic catalysts. Nature 1998;396(6709):353–6.
[6] Davis ME. Ordered porous materials for emerging applications. Nature 2002; 417(6891):813–21.
[7] Čejka J, Wichterlová B. Acid-catalyzed synthesis of mono- and dialkyl benzenes over zeolites: Active sites, zeolite topology, and reaction mechanisms. Catal Rev 2002;44(3):375–421.
[8] Corma A. State of the art and future challenges of zeolites as catalysts. J Catal 2003;216(1–2):298–312.
[9] Cundy CS, Cox PA. The hydrothermal synthesis of zeolites: History and development from the earliest days to the present time. Chem Rev 2003;103(3):663–702.
[10] Zones SI. Translating new materials discoveries in zeolite research to commercial manufacture. Microporous Mesoporous Mater 2011;144(1–3):1–8.
[11] Shi J, Wang Y, Yang W, Tang Y, Xie Z. Recent advances of pore system construction in zeolite-catalyzed chemical industry processes. Chem Soc Rev 2015;44(24):8877–903.
[12] Corma A. From microporous to mesoporous molecular sieve materials and their use in catalysis. Chem Rev 1997;97(6):2373–420.
[13] Amorim R, Vilaca N, Martinho O, Reis RM, Sardo M, Rocha J, et al. Zeolite structures loading with an anticancer compound as drug delivery systems. J Phys Chem C 2012;116(48):25642–50.
[14] Rimoli MG, Rabaioli MR, Melisi D, Curio A, Mondello S, Mirabelli R, et al. Synthetic zeolites as a new tool for drug delivery. J Bone Miner Res 2008;87A(1): 156–64.
[15] Dahm A, Eroksson H. Ultra-stable zeolites—A tool for in-cell chemistry. J Biotechnol 2004;111(3):279–90.
[16] Barrer RM. Synthesis of a zeolitic mineral with chabazite-like sorptive properties. J Chem Soc 1948;127–32.
[17] Kerr GT. Chemistry of crystalline aluminosilicates. II. The synthesis and properties of zeolite ZK-4. Inorg Chem 1966;5(9):1537–9.
[18] Schwochow F, Heinze G. Production of synthetic zeolites of faujasite structure. United States patent US 3720756. 1973 Mar 13.
[19] Puppe L, Schwochow F. Pure synthetic zeolite with faujasite structure—Made by pptn. and crystallisation of faujasite-aluminosilicate gels at 60–105 ºC. Deutsches patent DE 2605083. 1977 Aug 18.
[20] Barrer RM, Lee JA. Hydrocarbons in zeolite L: II. Entropy, physical state and isotherm model. Surf Sci 1968;12(2):354–68.
[21] Barrer RM. Syntheses and reactions of mordenite. J Chem Soc 1948:2158–63.
[22] Bertsch L, Habgood HW. An infrared spectroscopic study of the adsorption of water and carbon dioxide molecular sieve X. J Phys Chem 1963;67(8):1621–8.
[23] Howell PA. Low angle X-ray scattering from synthetic zeolites: Zeolites A, X and Y. J Phys Chem 1960;64(3):364–7.
[24] Habgood HW. Surface OH group on zeolite X. J Phys Chem 1965;69(5):1764–8.
[25] Nishimura Y. Synthesis and physico-chemical property of zeolite L. Japan J Chem 1970;91(23):1046–9. Japanese.
[26] Eberly PE Jr. Adsorption and separation of hydrocarbons on mordenite zeolites. Ind Eng Chem Prod Res Dev 1971;10(4):433–7.
[27] Baijpai PK, Rao MS, Gokhale KVGK. Synthesis of mordenite type zeolites. Ind Eng Chem Prod Res Dev 1978;17(3):223–7.
[28] Barrer RM, Denny PJ. Hydrothermal chemistry of the silicates. Part IX. Nitrogenous aluminosilicates. J Chem Soc 1961:971–82.
[29] Argauer RJ, Landolt GR. Crystalline zeolite ZSM-5 and method of preparing the same. United States patent US 3702886. 1972 Nov 14.
[30] Beck LW, Davis ME. Alkylammonium polycations as structure-directing agents in MFI zeolite synthesis. Microporous Mesoporous Mater 1998;22(1–3):107–14.
[31] Jia CJ, Masslani P, Bartjomeuf D. Characterization by infrared and nuclear magnetic resonance spectroscopies of calcined beta zeolite. J Chem Soc Faraday Trans 1993;89(19):3659–65.
[32] Pérez-Pariente J, Sanz J, Fornés V, Corma A. ^{29}Si and ^{27}Al MAS NMR study of zeolite β with different Si/Al rations. J Catal 1990;124(1):217–23.
[33] Pérez-Pariente J, Martens JA, Jacobs PA. Factors affecting the synthesis efficiency of zeolite beta from aluminosilicate gels containing alkali and tetraethylammonium ions. Zeolite 1988;8(1):46–53.
[34] Gao XT, Yeh CY, Angevine P. Mechanistic study of organic template removal from ZSM-5 precursors. Microporous Mesoporous Mater 2004;70(1–3):27–35.
[35] Oleksiak MD, Rimer JD. Synthesis of zeolites in the absence of organic structure-directing agents: Factors governing crystal selection and polymorphism. Rev Chem Eng 2014;30(1):1–49.
[36] Grose RW, Flanigen EM. Novel zeolite compositions and processes for preparing and using same. United States patent US 4257885. 1981 Mar 24.
[37] Li H, Xiang S, Wu D, Liu Y, Zhang X, Liu S. Study on the synthesis of zeolite ZSM-5. Chem J Chin Univ 1981;2(4):517–9. Chinese.
[38] Shiralkar VP, Clearfield A. Synthesis of the molecular sieve ZSM-5 without the aid of templates. Zeolite 1989;9(5):363–70.
[39] Narita E, Sato K, Yatabe N, Okabe T. Synthesis and crystal growth of zeolite ZSM-5 from sodium aluminosilicate systems free of organic templates. Ind Eng Chem Prod Res Dev 1985;24(4):507–12.
[40] Narayanan S, Sultana A, Krishna K, Mériaudeau P, Naccache C. Synthesis of ZSM-5 type zeolites with and without template and evaluation of physicochemical properties and aniline alkylation activity. Catal Lett 1995;34(1):129–38.
[41] Xie B, Song J, Ren L, Ji Y, Li J, Xiao F. Organotemplate-free and fast route for synthesizing beta zeolite. Chem Mater 2008;20(14):4533–5.
[42] Wang Y, Xiao F. Understanding mechanism and designing strategies for sustainable synthesis of zeolites: A personal story. Chem Rec 2016;16(3):1054–66.
[43] Corma A, Davis ME. Issues in the synthesis of crystalline molecular sieves: Towards the crystallization of low framework-density structures. ChemPhysChem 2004;5(3):304–13.
[44] De Moor PPEA, Beelen TPM, Komanschek BU, Bech LW, Wagner P, Davis ME, et al. Imaging the assembly process of the organic-mediated synthesis of a zeolite. Chemistry 1999;5(7):2083–8.
[45] Zhou Q, Li B, Qiu S, Pang W. Synthesis of low Si/Al β zeolite by using nucleation

gel. Chem J Chin Univ 1999;20(5):693–5. Chinese.
[46] Zhou Q, Qiu S, Pang W. Study on the crystallization mechanism of β zeolite synthesized with nucleation gel. Chem J Chin Univ 2000;21(1):1–4. Chinese.
[47] Xiong X, Fan F, Jun M, Li C, Liu S, Feng Z, et al. Fast crystallization of LTA zeolite from highly efficient NaY seed solution. Chem J Chin Univ 2007;28(1):21–5. Chinese.
[48] Xie B, Zhang H, Yang C, Liu S, Ren L, Zhang L, et al. Seed-directed synthesis of zeolites with enhanced performance in the absence of organic templates. Chem Commun 2011;47(13):3945–7.
[49] Zhang H, Xie B, Meng X, Müller U, Yilmaz B, Feyen M, et al. Rational synthesis of beta zeolite with improved quality by decreasing crystallization temperature in organotemplate-free route. Microporous Mesoporous Mater 2013;180:123–9.
[50] Otomo R, Yokoi T. Effect of the Al content in the precursor on the crystallization of OSDA-free beta zeolite. Microporous Mesoporous Mater 2016;224:155–62.
[51] Majano G, Delmotte L, Valtchev V, Mintova S. Al-rich zeolite beta by seeding in the absence of organic template. Chem Mater 2009;21(18):4184–91.
[52] Smith JV, Pluth JJ, Boqqs RC, Howard DG. Tschernichite, the mineral analogue of zeolite beta. J Chem Soc Chem Commun 1991;(6):363–4.
[53] Boggs RC, Howard DG, Smith JV, Klein GL. Tschernichite, a new zeolite from Goble, Columbia County, Oregon. Am Mineral 1993;78(7):822–6.
[54] Szostak R, Pan M, Lillerud KP. High-resolution TEM imaging of extreme faulting in natural zeolite tschernichite. J Phys Chem 1995;99(7):2104–9.
[55] De Ruite R, Famine K, Kentgens APM, Jansen JC, van Bekkum H. Synthesis of molecular sieve [B]-BEA and modification of the boron site. Zeolite 1993;13(8):611–21.
[56] Lohse U, Altrichter B, Donath R, Fricke R, Jancke K, Parlitz B, et al. Synthesis of zeolite beta. Part 1—Using tetraethylammonium hydroxide bromide with addition of chelates as templating agents. J Chem Soc Faraday Trans 1996;92(1):159–65.
[57] Camblor MA, Corma A, Iborra S, Miquel S, Primo J, Valencia S. Beta zeolite as a catalyst for the preparation of alkyl glucoside surfactants: The role of crystal size and hydrophobicity. J Catal 1997;172(1):76–84.
[58] Martinez-Franco R, Paris C, Martines-Armero ME, Martinez C, Moliner M, Corma A. High-silica nanocrystalline beta zeolites: Efficient synthesis and catalytic application. Chem Sci 2016;7(1):102–8.
[59] Borade RB, Clearfield AC. Synthesis of zeolite beta from dense system containing a minimum of template. Catal Lett 1994;26(3):285–9.
[60] Eapen MJ, Reddy KSN, Shiralkar VP. Hydrothermal crystallization of zeolite beta using tetraethylammonium bromide. Zeolite 1994;14(4):295–302.
[61] Van der Waal JC, Rigutto MS, van Bekkum H. Synthesis of all-silica zeolite beta. J Chem Soc, Chem Commun 1994;(10):1241–2.
[62] Kamimura Y, Chailittisilp W, Itabashi K, Shimojima A, Okubo T. Critical factors in the seed-assisted synthesis of zeolite beta and "green beta" from OSDA-free Na^+-aluminosilicate gels. Chem Asian J 2010;5(10):2182–91.
[63] Yokoi T, Yoshioka M, Imai H, Tatsumi T. Diversification of RTH-type zeolite and its catalytic application. Angew Chem Int Ed 2009;48(52):9884–7.
[64] Vortmann S, Marler B, Gies H, Daniels P. Synthesis and crystal structure of the new borosilicate zeolite RUB-13. Microporous Mater 1995;4(2–3):111–21.
[65] Liu M, Yokoi T, Yoshioka M, Imai H, Kondo JN, Tatsumi T. Differences in Al distribution and acidic properties between RTH-type zeolites synthesized with OSDAs and without OSDAs. Phys Chem Chem Phys 2014;16(9):4155–64.
[66] Kamimura Y, Itabashi K, Okubo T. Seed-assisted, OSDA-free synthesis of MTW-type zeolite and "green MTW" from sodium aluminosilicate gel systems. Microporous Mesoporous Mater 2012;147(1):149–56.
[67] Kamimura Y, Iyoki K, Elangovan SP, Itabashi K, Shimojima A, Okubo T. OSDA-free synthesis of MTW-type zeolite from sodium aluminosilicate gels with zeolite beta seeds. Microporous Mesoporous Mater 2012;163:282–90.
[68] Itabashi K, Kamimura Y, Iyoki K, Shimojima A, Okubo T. A working hypothesis for broadening framework types of zeolites in seed-assisted synthesis without organic structure-directing agent. J Am Chem Soc 2012;134(28):11542–9.
[69] Zhang H, Yang C, Zhu L, Meng X, Yilmaz B, Müller U, et al. Organotemplate-free and seed-directed synthesis of levyne zeolite. Microporous Mesoporous Mater 2012;155:1–7.
[70] Yang C, Ren L, Zhang H, Zhu L, Wang L, Meng X, et al. Organotemplate-free and seed-directed synthesis of ZSM-34 zeolite with good performance in methanol-to-olefins. J Mater Chem 2012;22(24):12238–45.
[71] Wu Q, Wang X, Meng X, Yang C, Liu Y, Jin Y, et al. Organotemplate-free, seed-directed, and rapid synthesis of Al-rich zeolite MTT with improved catalytic performance in isomerization of *m*-xylene. Microporous Mesoporous Mater 2014;186:106–12.
[72] Wang Y, Wang X, Wu Q, Meng X, Jin Y, Zhou X, et al. Seed-directed and organotemplate-free synthesis of TON zeolite. Catal Today 2014;226:103–8.
[73] Moller K, Bein T. Crystallization and porosity of ZSM-23. Microporous Mesoporous Mater 2011;143(2–3):253–62.
[74] Masih D, Kobayashi T, Baba T. Hydrothermal synthesis of pure ZSM-22 under mild conditions. Chem Commun 2007;(31):3303–5.
[75] Yoshioka M, Yokoi T, Liu M, Imai H, Inagaki S, Tatsumi T. Preparation of RTH-type zeolites with the amount and/or kind of organic structure-directing agents (OSDA): Are OSDAs indispensable for the crystallization. Microporous Mesoporous Mater 2012;153:70–8.
[76] Zhang L, Yang C, Meng X, Xie B, Wang L, Ren L, et al. Organotemplate-free syntheses of ZSM-34 zeolite and its heteroatom-substituted analogues with good catalytic performance. Chem Mater 2010;22(10):3099–107.
[77] Zhang H, Chu L, Xiao Q, Zhu L, Yang C, Meng X, et al. One-pot synthesis of Fe-beta zeolite by an organotemplate-free and seed-directed route. J Mater Chem A 2013;1(10):3254–7.
[78] Itakura M, Goto I, Takahashi A, Fujitani T, Ide Y, Sadakane M, et al. Synthesis of high-silica CHA type zeolite by interzeolite conversion of FAU type zeolite in the presence of seed crystals. Microporous Mesoporous Mater 2011;144(1–3):91–6.
[79] Yashiki A, Honda K, Fujimoto A, Shibata S, Ide Y, Sadakane M, et al. Hydrothermal conversion of FAU zeolite into LEV zeolite in the presence of non-calcined seed crystals. J Cryst Growth 2011;325(1):96–100.
[80] Honda K, Yashiki A, Itakura M, Ide Y, Sadakane M, Sano T. Influence of seeding on FAU–*BEA interzeolite conversions. Microporous Mesoporous Mater 2011;142(1):161–7.
[81] Honda K, Yashiki A, Sadakane M, Sano T. Hydrothermal conversion of FAU and *BEA-type zeolites into MAZ-type zeolites in the presence of non-calcined seed crystals. Microporous Mesoporous Mater 2014;196:254–60.
[82] Goel S, Zones SI, Iglesia E. Synthesis of zeolites via interzeolite transformations without organic structure-directing agents. Chem Mater 2015;27(6):2056–66.
[83] Zhang Z, Han Y, Xiao F, Qiu S, Zhu L, Wang R, et al. Mesoporous aluminosilicates with ordered hexagonal structure, strong acidity, and extraordinary hydrothermal stability at high temperatures. J Am Chem Soc 2001;123(21):5014–21.
[84] Liu J, Zhang X, Han Y, Xiao F. Direct observation of nanorange ordered microporosity within mesoporous molecular sieves. Chem Mater 2002;14(6):2536–40.
[85] Wu Z, Song J, Ji Y, Ren L, Xiao F. Organic template-free synthesis of ZSM-34 zeolite from an assistance of zeolite L seeds solution. Chem Mater 2008;20(22):357–9.
[86] Rubin MK, Rosinski EJ, Plank CJ. Hydrocarbon conversion with crystalline zeolite ZSM-34. United States patent US 4116813. 1978 Sep 26.
[87] Zhou F, Tian P, Liu Z, Liu G, Chang F, Li J. Synthesis of ZSM-34 and its catalytic properties in methanol-to-olefins reaction. Chin J Catal 2007;28(9):817–22.
[88] Vartuli JC, Kennedy GJ, Yoon BA, Malek A. Zeolite syntheses using diamines: Evidence for *in situ* directing agent modification. Microporous Mesoporous Mater 2000;38(2–3):247–54.
[89] Zhang H, Guo Q, Ren L, Yang C, Zhu L, Meng X, et al. Organotemplate-free synthesis of high-silica ferrierite zeolite induced by CDO-structure zeolite building units. J Mater Chem 2011;21(26):9494–7.
[90] Suzuki Y, Wakihara T, Itabashi K, Ogura M, Okubo T. Cooperative effect of sodium and potassium cations on synthesis of ferrierite. Top Catal 2009;52(1):67–74.
[91] Iyoki K, Takase M, Itabashi K, Muraoka K, Chaikittisilp W, Okubo T. Organic structure-directing agent-free synthesis of NES-type zeolites using EU-1 seed crystals. Microporous Mesoporous Mater 2015;215:191–8.
[92] Awala H, Gilson JP, Retoux R, Boullay P, Goupil JM, Valtchev V, et al. Template-free nanosized faujasite-type zeolites. Nat Mater 2015;14(4):447–51.
[93] Xie B. Seeded syntheses of zeolites in the absence of organic templates [dissertation]. Changchun: Jilin University; 2009. Chinese.
[94] Majano G, Darwiche A, Mintova S, Valtchev V. Seed-induced crystallization of nanosized Na-ZSM-5 crystals. Ind Eng Chem Res 2009;48(15):7084–91.
[95] Fan W, Shirato S, Gao F, Ogura M, Okubo T. Phase selection of FAU and LTA zeolites by controlling synthesis parameters. Microporous Mesoporous Mater 2006;89(1–3):227–34.
[96] Kapko V, Dawson C, Treacy MMJ, Thorpe MF. Flexibility of ideal zeolite frameworks. Phys Chem Chem Phys 2010;12(30):8531–41.
[97] Xu R, Pang W, Yu J, Huo Q, Chen J. Chemistry—Zeolite and porous material. Beijing: Science Press; 2004. Chinese.
[98] Zones SI. Zeolite SSZ-13 and its method of preparation. United States patent US 4544538. 1985 Oct 1.
[99] Zones SI. Conversion of faujasites to high-silica chabazite SSZ-13 in the presence of *N*,*N*,*N*-trimethyl-l-adamantammonium iodide. J Chem Soc Faraday Trans 1991;87(22):3709–16.
[100] Zones SI. Direct hydrothermal conversion of cubic P zeolite to organozeolite SSZ-13. J Chem Soc Faraday Trans 1990;86(20):3467–72.
[101] Wang X, Wu Q, Chen C, Pan S, Zhang W, Meng X, et al. Atom-economical synthesis of a high silica CHA zeolite using a solvent-free route. Chem Commun 2015;51(95):16920–3.
[102] Imai H, Hayashida N, Yokoi T, Tatsumi T. Direct crystallization of CHA-type zeolite from amorphous aluminosilicate gel by seed-assisted method in the absence of organic-structure-directing agents. Microporous Mesoporous Mater 2014;196:341–8.
[103] Ren L, Zhu L, Yang C, Chen Y, Sun Q, Zhang H, et al. Designed copper-amine complex as an efficient template for one-pot synthesis of Cu-SSZ-13 zeolite with excellent activity for selective catalytic reduction of NO_x by NH_3. Chem Commun 2011;47(35):9789–91.
[104] Wu Q, Wang X, Qi G, Pan S, Meng X, Xu J, et al. Sustainable synthesis of zeolite without addition of both organotemplates and solvents. J Am Chem Soc 2014;136(10):4019–25.
[105] Chen Z, Li S, Yan Y. Synthesis of template-free zeolite nanocrystals by reverse microemulsion-microwave method. Chem Mater 2005;17(9):2262–6.
[106] Wang Y, Sun Y, Mu Y, Zhang C, Li J, Yu J. Organotemplate-free hydrothermal synthesis of an aluminophosphate molecular sieve with AEN zeotype topology and properties of its derivatives. Chem Commun 2014;50(97):15400–3.
[107] Mu Y, Wang Y, Li Y, Yu J. Organotemplate-free synthesis of an open-framework magnesium aluminophosphate with proton conduction properties. Chem Commun 2015;51(11):2149–51.
[108] Sun Y, Yan Y, Wang Y, Li Y, Li J, Yu J. High proton conduction in a new alkali metal-templated open-framework aluminophosphate. Chem Commun 2015;51(45):9317–9.